The effects of Low-intensity Pulsed Ultrasound on tendon-bone healing in a transosseous-equivalent sheep rotator cuff model

Vedran Lovric, Michael Ledger, Jerome Goldberg, Wade Harper, Nicky Bertollo, Matthew H. Pelletier, Rema A. Oliver, Yan Yu & William R. Walsh

Knee Surgery, Sports Traumatology, Arthroscopy

ISSN 0942-2056

Knee Surg Sports Traumatol Arthrosc
DOI 10.1007/s00167-012-1972-z

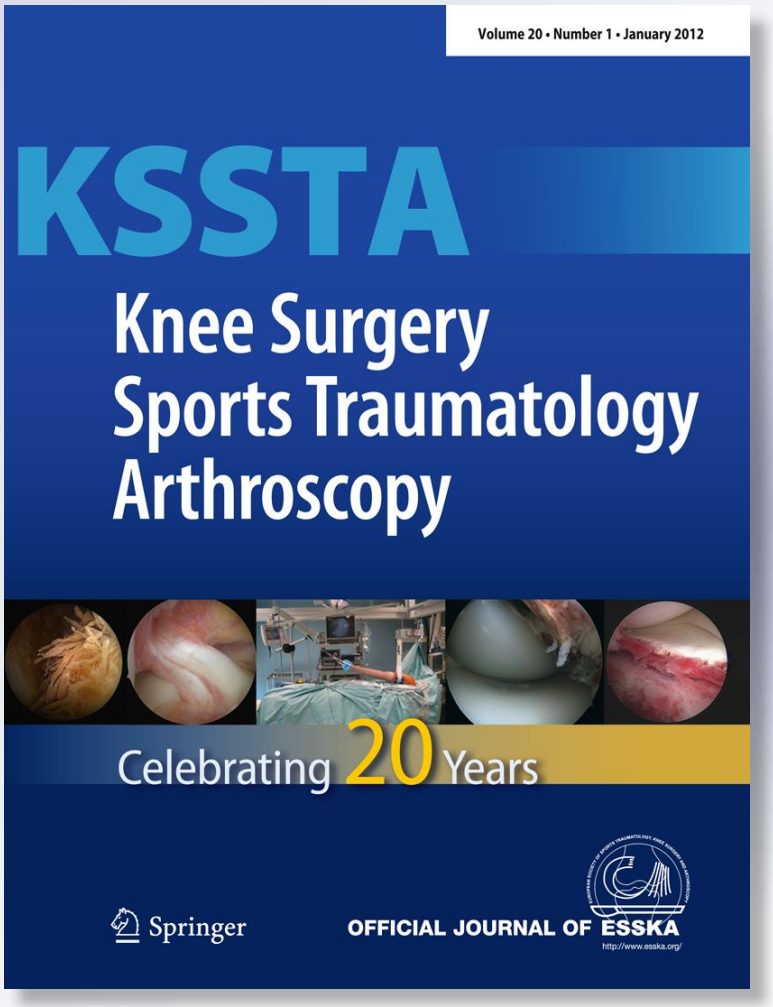

Springer

Knee Surg Sports Traumatol Arthrosc
DOI 10.1007/s00167-012-1972-z

EXPERIMENTAL STUDY

The effects of Low-intensity Pulsed Ultrasound on tendon-bone healing in a transosseous-equivalent sheep rotator cuff model

Vedran Lovric · Michael Ledger · Jerome Goldberg · Wade Harper · Nicky Bertollo · Matthew H. Pelletier · Rema A. Oliver · Yan Yu · William R. Walsh

Received: 7 September 2011 / Accepted: 15 March 2012

Abstract
Purpose The purpose of this study was to examine the effects Low-intensity Pulsed Ultrasound has on initial tendon-bone healing in a clinically relevant extra-articular transosseous-equivalent ovine rotator cuff model.
Methods Eight skeletally mature wethers, randomly allocated to either control group ($n = 4$) or treatment group ($n = 4$), underwent rotator cuff surgery following injury to the infraspinatus tendon. All animals were killed 28 days post surgery to allow examination of early effects of Low-intensity Pulsed Ultrasound treatment.
Results General improvement in histological appearance of tendon-bone integration was noted in the treatment group. Newly formed woven bone with increased osteoblast activity along the bone surface was evident. A continuum was observed between the tendon and bone in an interdigitated fashion with Sharpey's fibres noted in the treatment group. Low-intensity Pulsed Ultrasound treatment also increased bone mineral density at the tendon-bone interface ($p < 0.01$), while immunohistochemistry results revealed an increase in the protein expression patterns of VEGF ($p = 0.038$), RUNX2 ($p = 0.02$) and Smad4 ($p = 0.05$).
Conclusions The results of this study indicate that Low-intensity Pulsed Ultrasound may aid in the initial phase of tendon-bone healing process in patients who have undergone rotator cuff repair. This treatment may also be beneficial following other types of reconstructive surgeries involving the tendon-bone interface.

Keywords Tendon-bone healing · Low-intensity Pulsed Ultrasound · Rotator cuff repair · Entheses · Ovine model

Abbreviations

LIPUS	Low-intensity Pulsed Ultrasound
VEGF	Vascular endothelial growth factor
BMPs	Bone morphogenetic proteins
Micro-CT	Micro-computed tomography
H&E	Harris's haematoxylin and eosin
PBS-T	Phosphate-buffered saline with 0.2 % Tween-20
PBS	Phosphate-buffered saline
DAB	DAKO® liquid diaminobenzidine
IgG	Immunoglobulin
BMD	Bone mineral density

Introduction

Clinical scenarios related to entheses, attachment sites where tendons and ligaments meet bone, are usually associated with either tendinopathy or healing of the reattached tendon to bone following soft connective tissue reconstructive surgeries such as rotator cuff repair.

Rotator cuff surgery has seen vast improvements through the use of suture anchors and improved understanding of mechanical issues related to fixation techniques [8, 14, 20, 21, 31, 47]. Despite these advancements, numerous animal studies examining tendon to bone healing

Abstract originally presented at 57nd Annual Meeting of the Orthopaedic Research Society (ORS), Las Vegas, Nevada, January 13–16, 2011.

V. Lovric · M. Ledger · J. Goldberg · W. Harper · N. Bertollo · M. H. Pelletier · R. A. Oliver · Y. Yu · W. R. Walsh (✉)
Surgical and Orthopaedic Research Laboratories, Prince of Wales Clinical School, University of New South Wales, Sydney, NSW 2031, Australia
e-mail: W.Walsh@unsw.edu.au

Published online: 31 March 2012

have demonstrated that the overall structure, composition and organization of a typical, direct-type enthesis, characterized by a complex transitional structure consisting of four distinct zones, are not regenerated after repair [1–3, 17, 38, 46, 49]. This type of makeup facilitates the structure to function in unison and, in turn, allows for physiological loading and joint motion. It has been reported that rotator cuff healing occurs by gap scar formation [37, 48]. Furthermore, it is speculated that this is due to incomplete and abnormal expression of genes that naturally guide the development of the native tendon-bone interface [37]. More work is needed to accurately characterize the tendon-bone healing molecular pathways following rotator cuff repair.

Ultrasound has long been used in medicine as a diagnostic, therapeutic and surgical tool. It makes use of a noninvasive form of mechanical energy that is applied transcutaneously as acoustical pressure waves. Its application is largely dependent on levels of energy administered [40]. More recently, a new form of ultrasound, Low-intensity Pulsed Ultrasound (LIPUS), has received a great deal of attention from researchers and physicians alike. LIPUS delivers ultrasound energy of 30 mW/cm^2 at a high 1.5-MHz frequency in bursts of 200 μs and a duty cycle of 0.2. Benefits of using LIPUS have been well documented across all stages of bone healing, including angiogenesis, chondrogenesis and osteogenesis [40]. Accelerated healing has been reported in treatment for both fresh bone fractures and delayed unions and nonunions alike by superior endochondral ossification and osteoblast and fibroblast proliferation [6, 19, 24, 51]. In vitro experiments have shown ultrasound to increase cell proliferation, enhance collagen synthesis and significantly stimulate angiogenesis-related cytokines [10]. Subsequent in vitro experiments have demonstrated that LIPUS alters the differentiation pathway of the pluripotent mesenchymal cells into osteoblast and/or chondroblast lineage [22], stimulates osteogenic differentiation in osteoblastic cells [45] and, more recently, significantly increases the expression of bone morphogenetic protein (BMP) −2, −4 and −7 [43], which have been shown to directly participate in, and improve, tendon-bone healing [4, 37, 39, 52].

In vivo effects of LIPUS have also been reported. In an intra-articular sheep ACL reconstruction model, LIPUS treatment enhanced mechanical properties, increased cellular activity at the tendon-bone interface and accelerated the rate of angiogenesis [50]. Accelerated tendon-bone junction healing was also noted utilizing LIPUS in a partial patellectomy model in rabbits for periods up to 16 weeks. Results indicated accelerated and enhanced osteogenesis with superior mechanical properties in the LIPUS-treated animals [29, 34, 35].

The purpose of this study was to examine the effects of LIPUS on the early phases of tendon-bone healing in a clinically relevant, extra-articular transosseous-equivalent ovine rotator cuff model, which has not been evaluated previously. It was hypothesized that LIPUS, through alteration of critical molecular expressions, will accelerate and augment the early phases of tendon-bone healing process.

Materials and methods

Study approval was obtained from Animal Care and Ethics Committee of the University of New South Wales (ACEC Number: 10/110B).

Study design

Eight cross-bred wethers (18 months) underwent rotator cuff surgery to sever and reattach the infraspinatus tendon. Sheep were randomly allocated to either a LIPUS-treated group ($n = 4$) or a control group ($n = 4$) with no treatment. Animals were killed 28 days post surgery and histology, immunohistochemistry and micro-computed tomography endpoints performed to examine the early effects of LIPUS.

Animal model and surgery

Sheep were anesthetized and placed in the lateral position. Using the spine of scapula, acromion and the humeral head greater tuberosity as landmarks, an incision was made starting approximately three finger breadths beneath the outer one-third of the spine of scapula and passing between the lateral acromion and greater tuberosity of the humerus. Using blunt dissection, skin and subcutaneous tissues were elevated in the superior and inferior flaps. The brachial fascia was incised carefully in the line of the skin incision to expose the deltoideus muscle. The acromial head of the deltoideus was dissected along its superior or cranial edge. The acromial head of the deltoideus muscle was retracted inferiorly to expose the infraspinatus. The infraspinatus insertion was delineated by passing a curved artery forceps beneath its tendon as it inserts into the greater tuberosity. The infraspinatus tendon was sharply detached from its insertion into the greater tuberosity exposing the footprint of the muscles insertion (approximately 1 cm × 2 cm in size).

Cartilage at the footprint of the muscle insertion was burred to create a bleeding bone bed. The infraspinatus tendon was repaired with a transosseous-equivalent suture-bridge construct using medial row and lateral push-in suture anchors (Arthrex, Inc, Naples, Florida, USA).

Following surgery, animals were transferred to a cage and allowed to recover to a standing position while being observed.

Low-intensity Pulsed Ultrasound treatment

LIPUS treatment (30 mW/cm^2 delivered in 200-μs bursts of sine waves at a frequency of 1.5 MHz and a 0.2 duty cycle) was administered for the duration of 20 min per day until killing at day 28. The treatment protocol started the day following surgery and was administered 5 days per week continuously. The transducer (Melmak Ultrasound Device, Biomedical Tissue Technology Pty Ltd, Sydney, Australia) was placed over the surgical site and coupled to the skin using ultrasound gel.

Bone mineral density of newly formed bone (micro-computed tomography)

Micro-CT measurements revealed bone mineral density and micro-architecture of new bone formation. Bone mineral density is indicative of quality of healing between the tendon and bone.

Following retrieval, humeral head–infraspinatus tendon complex was scanned using micro-computed tomography (Siemens Inveon micro-CT System, Siemens Medical Solutions, Erlangen, Germany). Resulting effective pixel size of the scan measured 50.88 μm.

Scans were examined using MIMICS software (Mimics 12.0, Materialize, Belgium). The trans-axial midline of the tendon footprint was identified visually by aid of suture anchors in each sample. Five evenly spaced axial slices were evaluated for BMD measurement in five circular regions of interest (diameter (d) = 7 pixels) of each slice. Average BMD was taken across 5 slices.

Histology

After killing, humeral head–infraspinatus tendon complex was harvested and fixed for 48 h with 10 % neutral buffered formalin. Tissues were decalcified in 10 % formic acid-neutral buffered formalin solution, sectioned sagittally, parallel to the infraspinatus tendon insertion, and placed into cassettes ready for paraffin processing. Serial sections were cut at 5 microns thickness and stained with Harris's haematoxylin and eosin (H&E) for microscopic analysis of tissue morphology and cellular constituents. Histology was qualitatively graded for degree of tendon-bone integration, new bone formation, cellular activity and Sharpey's fibres. Specimens demonstrating increased tendon-bone integration, via inter-digitations and Sharpey's fibres, increased new bone formation and appropriate cellular activity were considered indicative of increased quality of tendon-bone healing. Collagen fibre alignment within healing tendons was evaluated using polarization microscopy. Higher levels of collagen fibre alignment and organization indicated a superior overall tendon quality at the interface and faster healing progression.

Immunohistochemistry

The immunohistochemistry procedure performed on the paraffin section to determine the expression of BMP-2, Smad4, VEGF and RUNX2 was derived from techniques previously reported [52, 53].

Briefly, slides were deparaffinized with xylene, rehydrated in a series of reduced concentrations of ethanol solutions. The slides were treated with a citrate-based (neutral pH) antigen retrieval solution (DAKO Pty Ltd, Glostrup, Denmark) at 95 °C for 20 min. Upon cooling to room temperature, endogenous peroxidase was quenched by 0.3 % hydrogen peroxide in 50 % methanol for 10 min. Slides were then rinsed in distilled water and washed in phosphate-buffered saline with 0.2 % Tween-20 (PBS-T). Primary mouse monoclonal antibodies against Smad4 (sc-7966), BMP-2 (sc-57040) and VEGF (sc-7269); rabbit polyclonal antibodies against RUNX2 (sc-10758) (Santa Cruz Biotechnology Inc, Santa Cruz, CA, USA); or non-immunized mouse and rabbit immunoglobulin (IgG) (DakoCytomation, Glostrup, Denmark), as negative controls, was applied to the sections (one antibody per section) and left overnight at 4 °C in humidity chambers. The concentrations of the primary antibodies used were 4 mg/ml for BMP-2 and RUNX2; 2 mg/ml for Smad4; and 1 mg/ml for VEGF. The final concentration of negative controls was 4 mg/ml.

The following day, the slides were washed three times in PBS-T, and the DakoCytomation Envision$^+$ System-HPR Labelled Polymer specific for mouse (K4001) or rabbit (K4003) (DakoCytomation, Glostrup, Denmark) was then applied at room temperature for 1 h. Sections were then washed in PBS-T four times prior to the application of a substrate–chromogen system, DAKO® Liquid diaminobenzidine (DAB) (K3468, DakoCytomation, Glostrup, Denmark). After 30 min, the reaction was terminated by immersing the slides in PBS. The sections were then counterstained with Harris's haematoxylin and mounted onto glass coverslips using EUKITT medium (Kindler GmbH & Co, Freiburg, Germany).

The immunohistochemical staining was assessed in a semiquantitative method by 3 observers in a blinded fashion. Two separate regions of interest fields (original magnification 10×) at each tendon-bone interface, which covered two-thirds of the tendon-bone interface, were assessed for each specimen and factor. Sections were graded for the proportion of cells that stained positively for the

Table 1 Grading system for immunohistochemical staining

	−	+	++	++	+++	+++	++++
Percentage of positively stained cells versus whole cell population	0	<10	25	Up to 50	50	Up to 80	>80
Staining intensity	No	Weak	Strong	Moderate	Strong	Moderate	Strong

marker versus the entire cell population at the tendon-bone interface as well as the staining intensity with reference to background staining. Cell phenotypes assessed included osteoblastic-like cells, osteoblast progenitor cells, proliferating fibroblasts and endothelial cells at the tendon-bone interface. A 5-grade scaling system was adapted with a combination of the percentage of cells stained and the staining intensity (Table 1).

Statistical analysis

BMD data and semiquantitative evaluation of BMP2, Smad4, VEGF and RUNX2 expression were analysed using SPSS version 18.0 (SPSS Inc, Chicago, Illinois). *T* test was performed, and statistical values of $p \leq 0.05$ were considered significant. Levene's test ($p \leq 0.05$) was used to confirm variance homogeneity of the populations.

Results

Surgery and LIPUS treatment was well tolerated by all animals. Placement of LIPUS sensor did not unsettle the animals. Upon harvest of tissue, neither infections nor tendon avulsions were recorded.

Histology

Histological appearance at the tendon-bone interface in LIPUS-treated group demonstrated general improvement in appearance compared to controls. Generally a thicker region of newly formed woven bone, morphologically resembling trabecular bone, with increased osteoblast activity along the bone surface, was noted at the tendon-bone interface in the LIPUS-treated group compared to the controls. The interface in the LIPUS-treated group revealed a continuum between the tendon and bone in an interdigitated fashion with noted Sharpey's fibres in contrast to the control group where discontinuous contact between the tendon and bone was observed (Fig. 1: control a, b, c; LIPUS d, e, f). Evidence of vascularization was noted by the presence of blood vessels.

Immunohistochemistry

All control sections showed only the blue colour of the Harris's haematoxylin counterstain, whereas the positive signals stained brown (Fig. 2).

Semiquantitative grading of immunohistochemical staining is summarized in Table 2, and representative images are shown in Fig. 3. Immunostaining of Smad4 was present in all cell types, while VEGF stained positive within osteoblasts, endothelial cells and some fibroblasts. Expression patterns or RUNX2 and BMP-2 were comparable (osteoblasts, osteoprogenitor cells and fibroblasts). Four weeks post surgery, there was no significant difference observed between the immunoreactivity of BMP-2 in the LIPUS-treated and the control groups. Immunostaining of Smad4, present in all cell types at the healing interface, was elevated ($p = 0.05$) in the LIPUS-treated group. Expression patterns of VEGF and RUNX2 both showed a significant difference (VEGF $p = 0.038$; RUNX2 $p = 0.02$) between the control and the LIPUS-treated groups.

Bone mineral density (micro-computed tomography)

Bone mineral density (BMD) at the footprint of the rotator cuff repair significantly increased in the LIPUS-treated group ($p < 0.01$) (Fig. 4).

Discussion

The most important finding of the present study was that LIPUS upregulates growth factor expression and healing of the tendon-bone interface compared to controls.

The current experimental study explored the effects of LIPUS application on the early phase of healing following an ovine rotator cuff repair using a clinically relevant transosseous-equivalent rotator cuff repair technique. Sheep animal model was chosen because of the previously reported size similarities between the human supraspinatus tendon and the sheep infraspinatus tendon [13, 16]. Traditionally the ovine rotator cuff animal model is associated with a distinct limitation in studying tendon-bone healing [42]. Immediate mechanical loading placed on the surgical repair postoperatively often results in detachment of the repaired tendon [37, 48] which does not mimic the

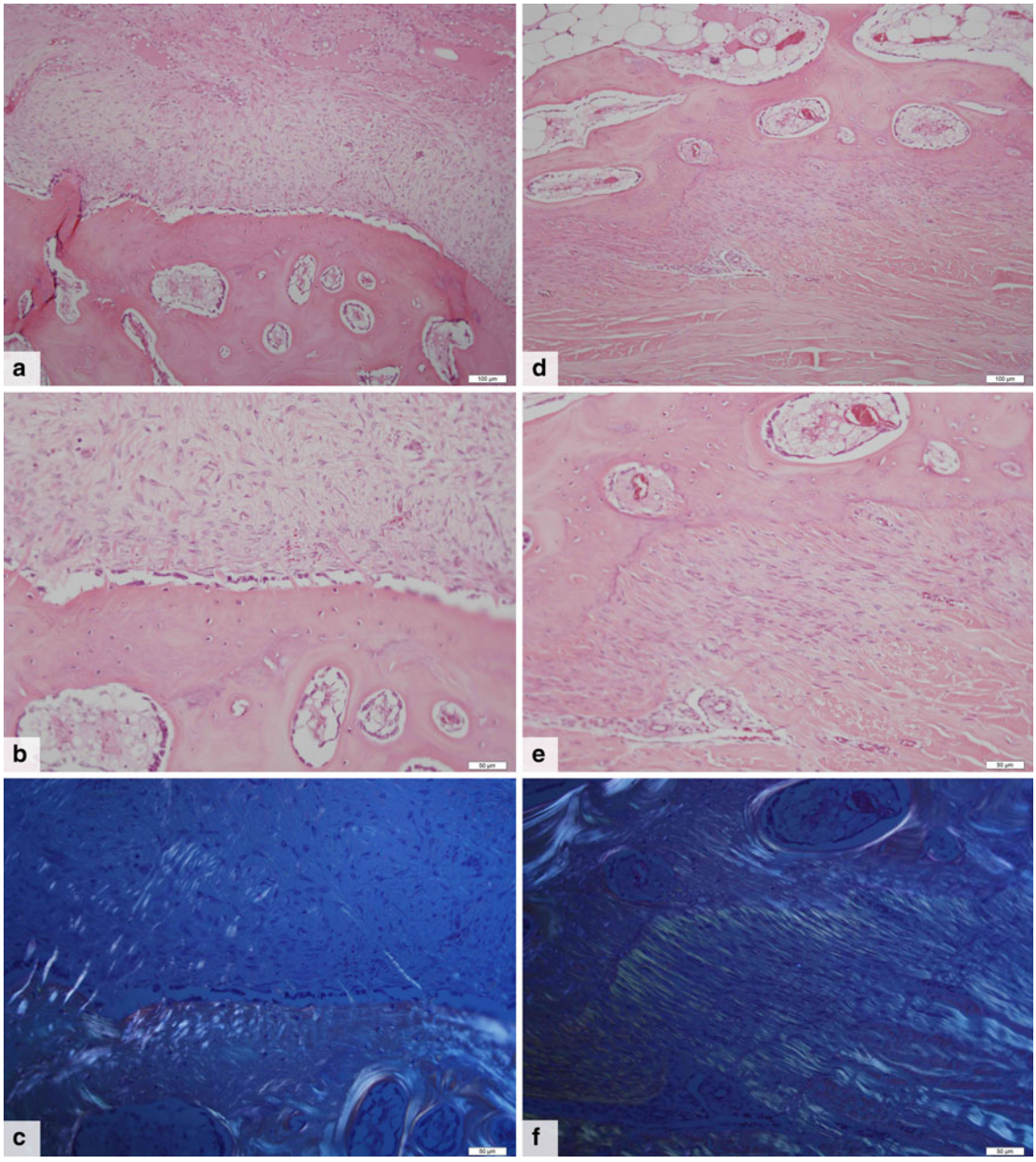

Fig. 1 Low-intensity Pulsed Ultrasound treatment group (**d** original magnification ×10; **e** original magnification ×20; **f** original magnification ×20 polarized light) at 4 weeks (H&E) showed a more organized and mature tendon-bone interface. Polarization microscopy revealed maturely aligned collagen fibres at the tendon-bone interface in all LIPUS-treated specimens, while the interface in the control specimens was made up of disorganized connective tissue layer (**a** original magnification ×10; **b** original magnification ×20; **c** original magnification ×20 polarized light)

tendon-bone healing following a rotator cuff repair in human subjects.

In order to avert the possibility of tendon detachment and potentially minimize gap formation, an ovine model that utilizes a 4-bridge transosseous-equivalent repair technique was developed [30]. This technique was shown to be more successful than the traditional single-row and double-row suture techniques. In a study by Park et al. [32], three different repair techniques were compared on fresh-frozen human cadaveric shoulders: 4-suture-bridge transosseous-equivalent; 2-suture-bridge transosseous-equivalent; and standard double-row. Pressurized contact area, mean pressure between the tendon and footprint, and the ultimate load to failure were recorded. The contact area for the 4-suture bridge was 115 mm^2; the 2-suture bridge was 91 mm^2; and the double-row was 56 mm^2. In an equivalent fashion, the pressure exerted by the 4-suture bridge was 0.27 MPa, the 2-suture bridge was 0.23 MPa, and the

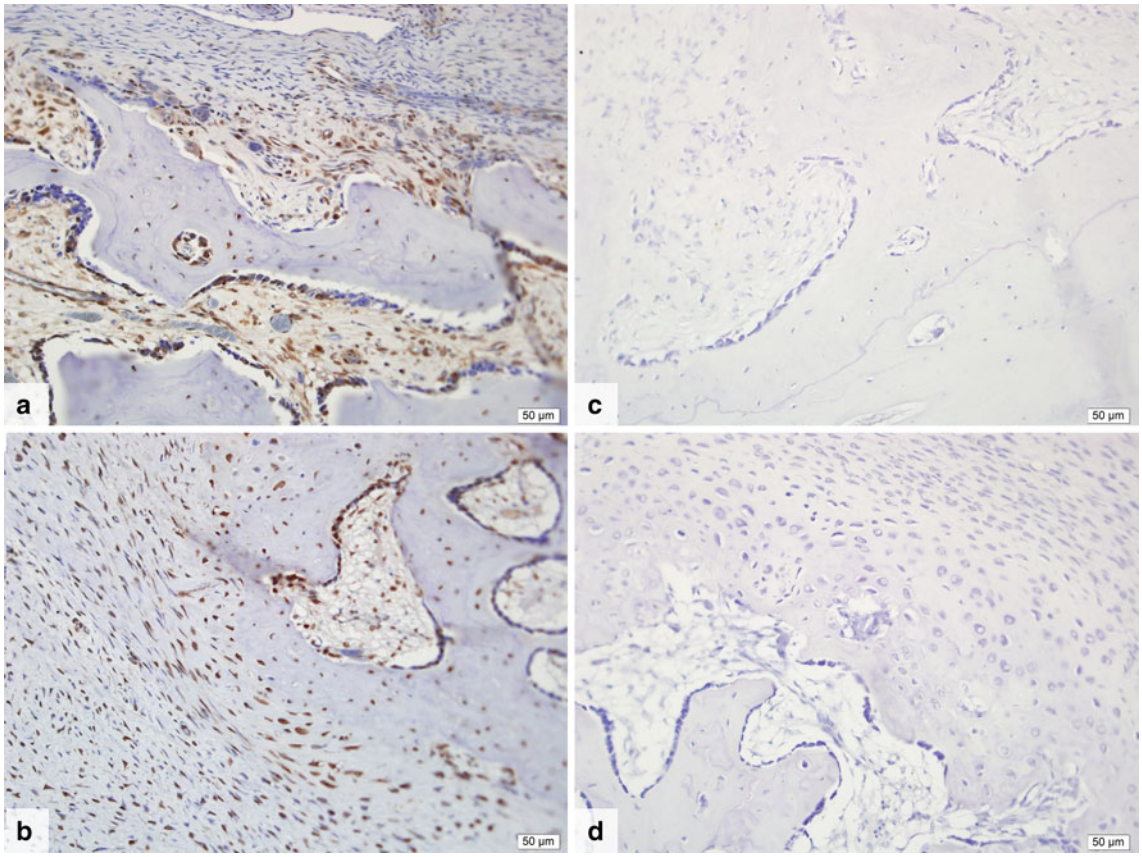

Fig. 2 Sections at 4 weeks post surgery stained with: **a** mouse monoclonal anti-Smad4 antibody; **b** rabbit polyclonal anti-RUNX2 antibody, and negative controls: **c** nonimmunized mouse IgG; **d** nonimmunized rabbit IgG (original magnification ×20)

Table 2 Results of semiquantitative evaluation of BMP-2, Smad4, VEGF and RUNX2 expression at 4-week time point

	Control	LIPUS
BMP-2	+/++	++/+++
Smad4	+/++	++/+++
VEGF	+	+++/++++
RUNX2	+	+++

double-row repair was 0.19 MPa [32]. The 4-suture bridge transosseous-equivalent repair technique provided a significantly increased biomechanical contact area and pressure over the footprint area, most closely restoring the native footprint and resulting in a minimal gap formation. Furthermore, the transosseous-equivalent repairs demonstrated significantly improved tensile loading properties when compared with double-row and single-row techniques. Ultimate load to failure ranging between 350 and 400 N was recorded for the transosseous-equivalent technique [33] compared to a load between 300 and 350 N for the double-row constructs and 275 to 300 N for the single-row repair technique [5].

Mechanisms that LIPUS, through mechanical stimulation of osteoblasts and fibroblasts, appears to pertain to healing at the tendon-bone junction revolves around the increased expression of angiogenic factor VEGF which plays an important role during angiogenesis [28, 35, 50], stimulation of osteogenic differentiation of mesenchymal stems cells [7, 26, 44], increase proliferation and differentiation of osteoblasts [10] and inhibit osteoclasts through regulation of their bone-resorbing activity [23, 25].

Blood supply is a key factor to any tissue healing after injury. Fealy et al. [12] evaluated vascularity after rotator

Fig. 3 Immunohistochemical staining of BMP-2 (**a** control; **e** LIPUS), ▶ Smad4 (**a** control; **f** LIPUS), VEGF (**c** control; **g** LIPUS) and RUNX2 (**d** control; **h** LIPUS) sections of the tendon-bone interface at 4 weeks post surgery (original magnification ×20). Expression patterns or RUNX2 and BMP-2 were comparable. Positive staining was observed in osteoblast-like cells and osteoprogenitor cells at the surface of the newly formed woven bone and in active fibroblasts found within the vicinity of the tendon-bone interface. Immunostaining of Smad4 was present in all cell types at the healing interface while VEGF stained positive within osteoblasts within newly formed bone, endothelial cells and some fibroblasts at the interface and focally within fibroblasts around the newly formed vessels. Significant difference was found in VEGF ($p = 0.038$), RUNX2 ($p = 0.02$) and Smad4 ($p = 0.05$) expressions between the two groups

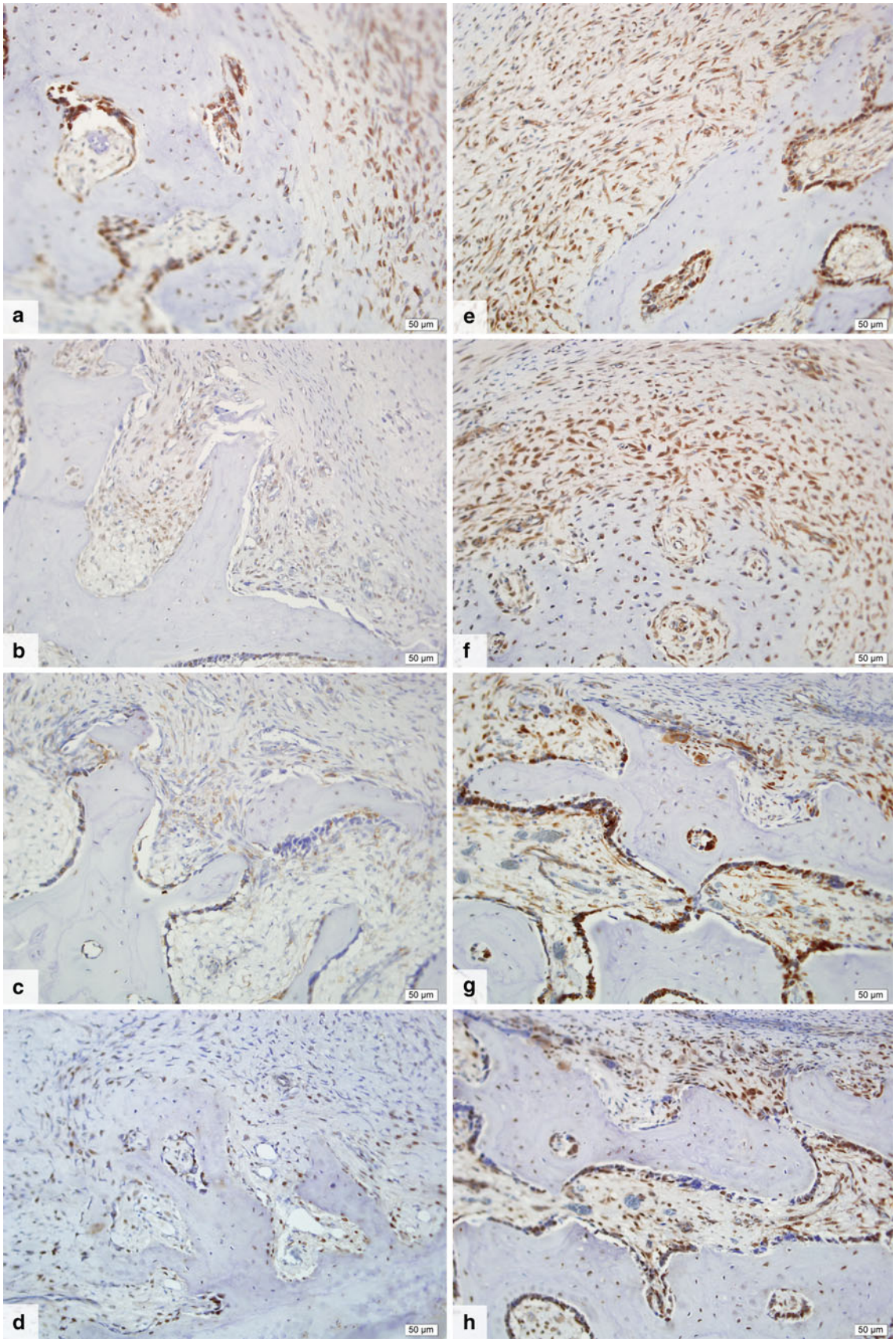

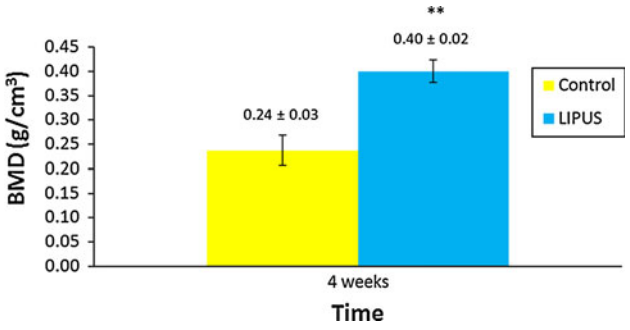

Fig. 4 Bone mineral density: control vs. LIPUS-treated groups; significant increase in bone mineral density ($p = 0.008$) at the tendon-bone interface was noted in the LIPUS-treated group compared to the control group at 4 weeks

cuff repair using contrast-enhanced power Doppler sonography and reported an increase immediately after repair confirming the popular belief that improved vascularity is detrimental in rotator cuff healing following repair. Similarly, adequate blood supply has been shown as a prerequisite for endochondral process of new bone formation [40] and for optimal bone regeneration [9]. The immunohistochemical results from this study indicated that the LIPUS-treated group expressed significantly stronger VEGF-positive signals compared to the control group, confirming claims that increased presence of VEGF plays a part in new bone formation.

Micro-CT was used to assess the bone mineral density within the newly formed bone at the footprint of the rotator cuff repair. It has been shown that increased mineral apposition rate and osteoid thickness, denoting intensified osteoblast activity, accelerate fracture healing of delayed unions [41] and improve the quality of tendon-to-bone interface [18]. Furthermore, Galatz et al. [15] demonstrated that bone loss at the tendon-to-bone insertion site significantly inhibits healing. It is hypothesized that this is due to the resorption of the bony surface collagen fibres that are prevented from incorporating into the mineralized tissue [36]. In this study, a biological effect was noted following a 4-week treatment with LIPUS. Micro-CT measurements revealed statistically greater BMD values and an increase in woven bone formation in the LIPUS-treated group. While this may suggest better healing in the LIPUS-treated animals, these results alone are not conclusive enough to insinuate a better-quality interface between the tendon and the bone.

The exact mechanisms that produce these biological effects in response to LIPUS treatment are not fully understood; however, the RUNX2 gene is considered to have the largest weighing in this complex healing process [11]. Recently, Suzuki et al. [44] reported that LIPUS significantly increases RUNX2 mRNA expression in rat osteoblasts in vitro. Suzuki et al. [43] also demonstrated that LIPUS can upregulate BMP-2, BMP-4 and BMP-5 in ROS 17/2.8 cells. Furthermore, BMP-2 has been found to upregulate RUNX2 mRNA expression in vitro [27]. In this study, immunohistochemical results showed a significant increase in RUNX2 expression in the LIPUS-treated group while no significant difference in BMP-2 expression at the 4-week time period between the treatment and control groups. In a study conducted by Yu et al. [52], it was found that BMP2 expression pattern in an ovine tendon-bone healing model, although present at the 6-week time period, peaked at its most functional period between 2 and 3 weeks post surgery. These findings may help explain why no differences were observed in this study at the 4-week time point.

Dose-dependant effects of LIPUS treatment were not assessed. Whether altered LIPUS signal parameters or longer treatment periods would be more effective is considered beyond the scope of this study. Further limitations of the study are that examinations were carried out at only one time point and that small animal numbers were used. Biomechanical testing was not performed; thus, the positive results could not be correlated to the strength of the interface. A 4-week time point was chosen to assess the effects of LIPUS in the early phases of healing. The results of this study confirm reports from previous in vitro and in vivo studies, suggesting that LIPUS improves tendon-bone healing by upregulating angiogenic and osteogenic pathways. Finally, this study examined tendon-bone healing following repair of a normal, healthy tendon; thus, the results are relevant to tendon-bone healing following repair of acute traumatic injury and may not translate directly to the same effects in a degenerated tendon after chronic tendon injury. Nonetheless, clinical application of LIPUS following repair of acute traumatic rotator cuff injuries may be beneficial.

Conclusion

LIPUS is a simple, feasible, noninvasive yet an economical treatment that has the potential to improve quality of repair following rotator cuff surgery.

Conflict of interest The authors declare that they have no conflict of interest.

Ethical Committee Animal Care and Ethics Committee of the University of New South Wales (ACEC Number: 10/110B).

References

1. Benjamin M, Kumai T, Milz S, Boszczyk BM, Boszczyk AA, Ralphs JR (2002) The skeletal attachment of tendons–tendon 'entheses'. Comp Biochem Physiol A Mol Integr Physiol 133(4): 931–945

2. Benjamin M, Toumi H, Ralphs JR, Bydder G, Best TM, Milz S (2006) Where tendons and ligaments meet bone: attachment sites ('entheses') in relation to exercise and/or mechanical load. J Anat 208(4):471–490
3. Carpenter JF, Thomopoulos S, Flanagan CL, DeBano CM, Soslowsky LJ (1998) Rotator cuff defect healing: a biomechanical and histologic analysis in an animal model. J Should Elbow Surg 7(6):599–605
4. Chen C-H, Liu H-W, Tsai C-L, Yu C-M, Lin IH, Hsiue G-H (2008) Photoencapsulation of bone morphogenetic protein-2 and periosteal progenitor cells improve tendon graft healing in a bone tunnel. Am J Sports Med 36(3):461–473
5. Cole BJ, ElAttrache NS, Anbari A (2007) Arthroscopic rotator cuff repairs: an anatomic and biomechanical rationale for different suture-anchor repair configurations. Arthroscopy 23(6): 662–669
6. Cook SD, Ryaby JP, McCabe J, Frey JJ, Heckman JD, Kristiansen TK (1997) Acceleration of tibia and distal radius fracture healing in patients who smoke. Clin Orthop Relat Res 337:198–207
7. Cui JH, Park K, Park SR, Min B-H (2006) Effects of low-intensity ultrasound on chondrogenic differentiation of mesenchymal stem cells embedded in polyglycolic acid: an in vivo study. Tissue Eng 12(1):75–82
8. Deakin M, Stubbs D, Bruce W, Goldberg J, Gillies RM, Walsh WR (2005) Suture strength and angle of load application in a suture anchor eyelet. Arthroscopy 21(12):1447–1451
9. Dimitriou R, Tsiridis E, Giannoudis PV (2005) Current concepts of molecular aspects of bone healing. Injury 36(12):1392–1404
10. Doan N, Reher P, Meghji S, Harris M (1999) In vitro effects of therapeutic ultrasound on cell proliferation, protein synthesis, and cytokine production by human fibroblasts, osteoblasts, and monocytes. J Oral Maxillofac Surg 57(4):409–419
11. Ducy P, Zhang R, Geoffroy V, Ridall AL, Karsenty G (1997) Osf2/Cbfa1: a transcriptional activator of osteoblast differentiation. Cell 89(5):747–754
12. Fealy S, Adler RS, Drakos MC (2006) Patterns of vascular and anatomical response after rotator cuff repair. Am J Sports Med 34(1):120–127
13. France EP, Paulos LE, Harner CD, Straight CB (1989) Biomechanical evaluation of rotator cuff fixation methods. Am J Sports Med 17(2):176–181
14. Franceschi F, Ruzzini L, Longo UG, Martina FM, Beomonte Zobel B, Maffulli N, Denaro V (2007) Equivalent clinical results of arthroscopic single-row and double-row suture anchor repair for rotator cuff tears: a randomized controlled trial. Am J Sports Med 35(8):1254–1260
15. Galatz LM, Rothermich SY, Zaegel M, Silva MJ, Havlioglu N, Thomopoulos S (2005) Delayed repair of tendon to bone injuries leads to decreased biomechanical properties and bone loss. J Orthop Res 23(6):1441–1447
16. Gerber C, Schneeberger A, Beck M, Schlegel U (1994) Mechanical strength of repairs of the rotator cuff. J Bone Jt Surg Br 76-B (3):371–380
17. Gerber C, Schneeberger AG, Perren SM, Nyffeler RW (1999) Experimental rotator cuff repair. a preliminary study. J Bone Jt Surg Am 81(9):1281–1290
18. Hays PL, Kawamura S, Deng XH, Dagher E, Mithoefer K, Liang Y, Rodeo SA (2008) The role of macrophages in early healing of a tendon graft in a bone tunnel. J Bone Jt Surg Am 90(3):565–579
19. Heckman J, Ryaby J, McCabe J, Frey J, Kilcoyne R (1994) Acceleration of tibial fracture-healing by non-invasive, low-intensity pulsed ultrasound. J Bone Jt Surg Am 76(1):26–34
20. Hughes P, Miller B, Goldberg J, Sonnabend D, Fullilove S, Evans R, Gilles S, Walsh W (2003) Effect of limb orientation and traction on the tendon bone interface. J Bone Jt Surg Br 85-B (SUPP_I):68
21. Hughes PJ, Evans RON, Miller B, Goldberg J, Sonnabend DH, Walsh WR (2005) Boundary conditions at the tendon-bone interface. Knee Surg Sports Traumatol Arthrosc 13(1):55–59
22. Ikeda K, Takayama T, Suzuki N, Shimada K, Otsuka K, Ito K (2006) Effects of low-intensity pulsed ultrasound on the differentiation of C2C12 cells. Life Sci 79(20):1936–1943
23. Kochanowska I, Chaberek S, Wojtowicz A, Marczynski B, Wlodarski K, Dytko M, Ostrowski K (2007) Expression of genes for bone morphogenetic proteins BMP-2, BMP-4 and BMP-6 in various parts of the human skeleton. BMC Musculoskelet Disord 8(1):128
24. Kristiansen TK, Ryaby JP, Mccabe J, Frey JJ, Roe LR (1997) Accelerated healing of distal radial fractures with the use of specific, low-intensity ultrasound. A multicenter, prospective, randomized, double-blind, placebo-controlled study. J Bone Jt Surg Am 79(7):961–973
25. Lee HJ, Choi BH, Min BH, Park SR (2007) Low-intensity ultrasound inhibits apoptosis and enhances viability of human mesenchymal stem cells in three-dimensional alginate culture during chondrogenic differentiation. Tissue Eng 13(5):1049–1057
26. Lee HJ, Choi BH, Min BH, Son YS, Park SR (2006) Low-intensity ultrasound stimulation enhances chondrogenic differentiation in alginate culture of mesenchymal stem cells. Artif Organs 30(9):707–715
27. Lee MH, Javed A, Kim HJ, Shin HI, Gutierrez S, Choi JY, Rosen V, Stein JL, van Wijnen AJ, Stein GS, Lian JB, Ryoo HM (1999) Transient upregulation of CBFA1 in response to bone morphogenetic protein-2 and transforming growth factor β1 in C2C12 myogenic cells coincides with suppression of the myogenic phenotype but is not sufficient for osteoblast differentiation. J Cell Biochem 73(1):114–125
28. Lu H, Qin L, Cheung W, Lee K, Wong W, Leung K (2008) Low-intensity pulsed ultrasound accelerated bone-tendon junction healing through regulation of vascular endothelial growth factor expression and cartilage formation. Ultrasound Med Biol 34(8): 1248–1260
29. Lu H, Qin L, Fok P, Cheung W, Lee K, Guo X, Wong W, Leung K (2006) Low-intensity pulsed ultrasound accelerates bone-tendon junction healing: a partial patellectomy model in rabbits. Am J Sports Med 34(8):1287–1296
30. Maguire M, Goldberg J, Bokor D, Bertollo N, Pelletier M, Harper W, Walsh W (2011) Biomechanical evaluation of four different transosseous-equivalent/suture bridge rotator cuff repairs. Knee Surg Sports Traumatol Arthrosc 19(9):1582–1587
31. Meier SW, Meier JD (2006) Rotator cuff repair: the effect of double-row fixation on three-dimensional repair site. J Should Elbow Surg 15(6):691–696
32. Park MC, ElAttrache NS, Tibone JE, Ahmad CS, Jun B-J, Lee TQ (2007) Part I: footprint contact characteristics for a transosseous-equivalent rotator cuff repair technique compared with a double-row repair technique. J Should Elbow Surg 16(4):461–468
33. Park MC, Tibone JE, ElAttrache NS, Ahmad CS, Jun B-J, Lee TQ (2007) Part II: biomechanical assessment for a footprint-restoring transosseous-equivalent rotator cuff repair technique compared with a double-row repair technique. J Should Elbow Surg 16(4):469–476
34. Qin L, Fok P, Lu H, Shi S, Leng Y, Leung K (2006) Low intensity pulsed ultrasound increases the matrix hardness of the healing tissues at bone-tendon insertion: a partial patellectomy model in rabbits. Clin Biomech 21(4):387–394
35. Qin L, Lu H, Fok P, Cheung W, Zheng Y, Lee K, Leung K (2006) Low-intensity pulsed ultrasound accelerates osteogenesis at bone-tendon healing junction. Ultrasound Med Biol 32(12):1905–1911

36. Rodeo S, Arnoczky S, Torzilli P, Hidaka C, Warren R (1993) Tendon-healing in a bone tunnel. A biomechanical and histological study in the dog. J Bone Jt Surg Am 75(12):1795–1803
37. Rodeo SA (2007) Biologic augmentation of rotator cuff tendon repair. J Should Elbow Surg 16 (5, Suppl 1):S191–S197
38. Rodeo SA, Potter HG, Kawamura S, Turner AS, Kim HJ, Atkinson BL (2007) Biologic augmentation of rotator cuff tendon-healing with use of a mixture of osteoinductive growth factors. J Bone Jt Surg Am 89(11):2485–2497
39. Rodeo SA, Suzuki K, Deng X-h (1999) Use of recombinant human bone morphogenetic protein-2 to enhance tendon healing in a bone tunnel. Am J Sports Med 27(4):476–488
40. Rubin C, Bolander M, Ryaby JP, Hadjiargyrou M (2001) The use of low-intensity ultrasound to accelerate the healing of fractures. J Bone Jt Surg Am 83-A (2):259–270
41. Rutten S, Nolte PA, Korstjens CM, van Duin MA, Klein-Nulend J (2008) Low-intensity pulsed ultrasound increases bone volume, osteoid thickness and mineral apposition rate in the area of fracture healing in patients with a delayed union of the osteotomized fibula. Bone 43(2):348–354
42. Soslowsky LJ, Carpenter JE, DeBano CM, Banerji IB, Moalli MR (1996) Development and use of an animal model for investigations on rotator cuff disease. J Should Elbow Surg 5(5): 383–392
43. Suzuki A, Takayama T, Suzuki N, Kojima T, Ota N, Asano S, Ito K (2009) Daily low-intensity pulsed ultrasound stimulates production of bone morphogenetic protein in ROS 17/2.8 cells. J Oral Sci 51(1):29–36
44. Suzuki A, Takayama T, Suzuki N, Sato M, Fukuda T, Ito K (2009) Daily low-intensity pulsed ultrasound-mediated osteogenic differentiation in rat osteoblasts. Acta Biochim Biophys Sin 41(2):108–115
45. Takayama T, Suzuki N, Ikeda K, Shimada T, Suzuki A, Maeno M, Otsuka K, Ito K (2007) Low-intensity pulsed ultrasound stimulates osteogenic differentiation in ROS 17/2.8 cells. Life Sci 80(10):965–971
46. Thomopoulos S, Hattersley G, Rosen V, Mertens M, Galatz L, Williams GR, Soslowsky LJ (2002) The localized expression of extracellular matrix components in healing tendon insertion sites: an in situ hybridization study. J Orthop Res 20(3):454–463
47. Tuoheti Y, Itoi E, Yamamoto N (2005) Contact area, contact pressure, and pressure patterns of the tendon-bone interface after rotator cuff repair. Am J Sports Med 33(12):1869–1874
48. Turner AS (2007) Experiences with sheep as an animal model for shoulder surgery: strengths and shortcomings. J Should Elbow Surg 16 (5, Suppl 1):158–163
49. Walsh WR, Harrison JA, Van Sickle D (2004) Patellar tendon-to-bone healing using high-density collagen bone anchor at 4 years in a sheep model. Am J Sports Med 32(1):91–95
50. Walsh WR, Stephens P, Vizesi F, Bruce W, Huckle J, Yu Y (2007) Effects of low-intensity pulsed ultrasound on tendon-bone healing in an intra-articular sheep knee model. Arthroscopy 23(2):197–204
51. Warden SJ (2003) A new direction for ultrasound therapy in sports medicine. Sports Med 33:95–107
52. Yu Y, Bliss JP, Bruce WJM, Walsh WR (2007) Bone morphogenetic proteins and smad expression in ovine tendon-bone healing. Arthroscopy 23(2):205–210
53. Yu Y, Yang JL, Chapman-Sheath PJ, Walsh WR (2002) TGF-β, BMPS, and their signal transducing mediators, Smads, in rat fracture healing. J Biomed Mater Res 60(3):392–397